

# Application of Simulated Annealing for Color Pattern Recognition to the Optoelectronic Correlator with Liquid Crystal Device

Sihliang Fu, Chulung Chen\*, Weichih Liao, Yunghsin Hsu, and Chengsyuan You

**Abstract**—A procedure using stimulated annealing algorithm to design the reference function is proposed. First we encode color pattern into a single channel and use the minimum average correlation energy to obtain an initial feasible solution and the state. Then we substitute the solution into stimulated annealing algorithm to obtain the optimizing reference function, and utilize the multilevel quantitative analysis of the reference function. Finally we utilize Mach-Zehnder joint transform correlator with simulated annealing to obtain the optimization of the reference function for recognition of color targets. From numerical results, the performance is accepted.

**Index Terms**—minimum average correlation energy, simulated annealing, color pattern recognition, Mach-Zehnder joint transform correlator

## I. INTRODUCTION

In 1964, VanderLugt proposed the concept of matching spatial filter device, called VanderLugt correlator (VLC) [1]. The optical correlator only identified graphics with shift invariance, but not rotation invariance. In 1966, Weaver and Goodman [2] improved the VLC by proposing the joint transform correlator (JTC) for pattern recognition application. But there are still some problems in the JTC structure. The main one in the structure is that the energy of zero-order term (also called DC term) is too tremendous. The DC term is the sum of each auto-correlation of the reference image and the target image at the output of correlation plane. The value of the DC term will influence the detected signal accuracy, so the removal of the nonzero-order term (N0JTC) is of great importance.

Lu et al. [3] utilized phase-shifting technique to design a nonzero-order JTC (N0JTC) and Li et al. [4] used the joint transform power spectrum (JTPS) subtraction strategy to realize the N0JTC. The Mach-Zehnder JTC (MZJTC) [5] can

remove the zero-order term in only one step directly without storing the Fourier spectra of both the reference and target images beforehand. Later, Chen et al. [6,7] adopted minimum average correlation energy (MACE) to yield a sharp correlation peak.

On the other hand, Kirkpatrick et al. [8] proposed the simulated annealing and successfully applied it to optimization problems. Annealing is a physical process of decreasing temperature slowly in order to reach the global minimum energy states. We will take advantage of this feature in this research.

## II. ANALYSIS

The MZJTC structure is shown in Fig. 1. It includes a laser, one spatial filter, one collimated lens (CL), three beam splitters (BS), three polarizing beam splitters (PBS), three Fourier lenses (FL), three reflective liquid spatial light modulators (RLCSLM), three charge coupled device (CCD) cameras, one electronic subtractor (ES) which is used for removing the zero-order term of JTPS, and one computer for controlling the whole system. There are one half wave plate (HWP) and one quarter wave plate (QWP) in front of each RLCSLM. The MZJTC structure is based on the Mach-Zehnder interferometer technique with Stokes relationships. The difference between N0JTC and MZJTC is the MZJTC structure only needs one step to remove the zero-order term of JTPS. The processes are presented as follows.

We arrange the locations of the target image and the reference image at the RLCSLM1 and the RLCSLM2, respectively, where  $(x, y)$  denote the coordinates of input planes, and  $b$  is the distance from the horizontal center of the origin of coordinates.

Let  $t$  and  $r$  be the transmission and reflection coefficients of the beam splitter for light incident from FL1, and  $r'$  and  $t'$  be the corresponding values of light incident from FL2. The target on the RLCSLM1 is illuminated and Fourier optically transformed by FL1. Passing through the BS3, the irradiation of transmitted and reflected Fourier spectrum is respectively detected by CCD1 and CCD2 in the frequency domain. In the same way, the reference on the RLCSLM2 is illuminated and Fourier optically transformed

Manuscript received January 18, 2012. This work was supported by the National Science Council in Taiwan, under Grant No. NSC 100-2221-E-155-044.

Sihliang Fu is with the department of Photonics Engineering, Yuan Ze university, 135 Yung Tung Road, Taoyuan 32026, Taiwan.

Chulung Chen is with the Department of Photonics Engineering, Yuan Ze university, 135 Yung Tung Road, Taoyuan 32026, Taiwan. (Corresponding author. Phone: +886-3-4638800 ext 7513; Fax: +886-3-4639355; E-mail: chulung@saturn.yzu.edu.tw).

Weichih Liao is with the Department of Photonics Engineering, Yuan Ze university, 135 Yung Tung Road, Taoyuan 32026, Taiwan.

Yunghsin Hsu is with the Department of Photonics Engineering, Yuan Ze university, 135 Yung Tung Road, Taoyuan 32026, Taiwan.

Chengsyuan You is with the Department of Photonics Engineering, Yuan Ze university, 135 Yung Tung Road, Taoyuan 32026, Taiwan.

by FL2, and the transmitted and reflected Fourier spectrum is respectively detected by CCD2 and CCD1. Then, the summation of spectra on CCD1 is

$$P_1(u, v) = \tau \cdot |F(u, v)| \cdot \exp[-j2\pi bu] \cdot \exp[j\theta_1(u, v)] + r' \cdot |H(u, v)| \cdot \exp[j2\pi bu] \cdot \exp[j\theta_2(u, v)]. \quad (1)$$

Similarly, the summation of spectra on CCD2 is

$$P_2(u, v) = \tau' \cdot |H(u, v)| \cdot \exp[j2\pi bu] \cdot \exp[j\theta_2(u, v)] + r \cdot |F(u, v)| \cdot \exp[-j2\pi bu] \cdot \exp[j\theta_1(u, v)]. \quad (2)$$

Here  $|F(u, v)|$  and  $|H(u, v)|$  represent the modules of the Fourier spectrum of the target and reference, respectively,  $\theta_1(u, v)$  and  $\theta_2(u, v)$  are the corresponding phases of Fourier spectra.  $u$  and  $v$  denote the spatial frequency coordinate at the CCD plane. The resultant irradiation on CCD1 can be written as

$$I_1(u, v) = |P_1(u, v)|^2 = \tau^2 \cdot |F(u, v)|^2 + r'^2 \cdot |H(u, v)|^2 + t(r')^* |F(u, v)| |H(u, v)| \cdot \exp(-j[2\pi(2b)u + \theta_2(u, v) - \theta_1(u, v)]) + r't^* |H(u, v)| |F(u, v)| \cdot \exp[j2\pi(2b)u + \theta_2(u, v) - \theta_1(u, v)]. \quad (3)$$

Similarly, the joint Fourier power spectrum in frequency plane  $P_2$  on CCD2 also can be written as

$$I_2(u, v) = |P_2(u, v)|^2 = r^2 \cdot |F(u, v)|^2 + t'^2 \cdot |H(u, v)|^2 + r(t')^* |F(u, v)| |H(u, v)| \cdot \exp(-j[2\pi(2b)u + \theta_2(u, v) - \theta_1(u, v)]) + t'r^* |H(u, v)| |F(u, v)| \cdot \exp(j[2\pi(2b)u + \theta_2(u, v) - \theta_1(u, v)]). \quad (4)$$

Here the superscript  $*$  denotes the complex conjugate. In order to obtain the nonzero-order term, we sent the outputs of CCD1 and CCD2 to the ES, the resultant output of ES becomes

$$I_s = I_2 - I_1 = (r^2 - \tau^2) \cdot |F(u, v)|^2 + (t'^2 - r'^2) \cdot |H(u, v)|^2 + [r(t')^* - t(r')^*] |F(u, v)| |H(u, v)| \cdot \exp(-j[2\pi(2b)u + \theta_2(u, v) - \theta_1(u, v)]) + [t'r^* - r't^*] |H(u, v)| |F(u, v)| \cdot \exp[j2\pi(2b)u + \theta_2(u, v) - \theta_1(u, v)]. \quad (5)$$

Here  $I_s$  denotes the difference of joint Fourier power spectrum between CCD1 and CCD2. Using the Stokes relationships ( $t = t'$ ,  $r = -r'$ ,  $t^*r' + r^*t = 0$ ), we obtain

$$I_s = (r^2 - \tau^2) \cdot |F(u, v)|^2 + (t'^2 - r'^2) \cdot |H(u, v)|^2 + 4|F(u, v)| |H(u, v)| \cdot \text{Re}\{rt^* \cdot \exp(-j[2\pi(2b)u + \theta_2(u, v) - \theta_1(u, v)])\}. \quad (6)$$

Here  $\text{Re}\{\cdot\}$  takes the real part. Assume the BS is 50/50 (i.e.,  $|r| = |t| = |r'| = |t'| = 1/2$ ), Eq.(23) can be rewritten as

$$I_s = |F(u, v)| |H(u, v)| \cos[2\pi(2b)u + \theta_2(u, v) - \theta_1(u, v)]. \quad (7)$$

In Eq. (7) the difference signal  $I_s$  acts like a nonzero-order joint power spectrum (N0JPS), because the  $|F(u, v)|^2$  and  $|H(u, v)|^2$  have been removed. After inverse Fourier transform, the N0JPS becomes only cross-correlation terms and appears in the output correlation plane on CCD3 as

$$c(x, y) = f(x, y) \otimes h(x, y) \oplus \delta(x - 2b, y) + h(x, y) \otimes f(x, y) \oplus \delta(x + 2b, y). \quad (8)$$

Here  $\otimes$  and  $\oplus$  denote correlation and convolution, respectively;  $\delta(x, y)$  is the delta function. Eq. (8) shows that two same size cross-correlation terms are produced at  $(x \pm 2b, y)$ . The output  $c(x, y)$  achieves the nonzero-order joint transform correlation.

With the observation on the correlation output at the output plane, some measurement criteria [9] for evaluating the recognition ability are defined as follows:

1. Correlation peak intensity (CPI)

The CPI is the cross-correlation peak intensity at the correlation output plane.

$$CPI = |c(o, o)|^2 \tag{9}$$

Here (0, 0) is the central position of desired cross-correlation peak

2. Peak to sidelobe ratio (PSR)

PSR is the desired correlation peak energy versus sidelobes energy on the correlation output plane, which is expressed as

$$PSR = \frac{|c(o, o)|^2}{\max_{x, y \in \Omega} \{|c(x, y)|^2\}} \tag{10}$$

Here  $\Omega = \{(x, y) \mid |x| > 2, |y| > 2\}$ .

3. Correlation energy to Peak Energy ratio (CPE)

CPE [10] is the output of correlation plane energy versus CPI. It is expressed as

$$CPE = \frac{\sum_x \sum_y |c(x, y)|^2}{|c(o, o)|^2} \tag{11}$$

Here  $|c(0,0)|^2$  is CPI,  $\sum_x \sum_y |c(x, y)|^2$  is the total correlation plane energy. This criterion is the major measurement in our study.

### III. NUMERICAL PROCESS

We choose a colorful tropical fish to be the original image, whose size is of  $64 \times 64 \times 3$  pixels. It will be separated into R、G、B channels. We encoded R、G、B of the image into a single channel from the target image. New size of the image is of  $192 \times 64$  pixels. It is shown in Fig. 2. We rotate the new image from  $-14^\circ$  to  $14^\circ$ , and select one image for each two degrees. Totally there are 15 pictures used as training images. In the beginning, we utilize the training set to produce an initial reference function from MACE technique for a better starting solution with SA. In the SA procedure we use 3 different level numbers on reference functions for comparative analysis.

In our study, we proposed the use of CPE to be a criterion which corresponds to the energy function of SA algorithm for recognition.

There are nine steps in SA algorithm described as follows.

1. Yield the initial stratification reference function from MACE technique.

2. Calculate CPE for each training image, and add all CPEs as the energy function. It is expressed as

$$E_{old} = \sum_{i=1}^N CPE_i^2 \tag{12}$$

Here  $i$  is the number of training image corresponds to CPE

3. Alter the level number just for one pixel of the reference function  $h(x, y)$ , and then calculate the new energy function  $E_{new}$ .

4. If the minimum peak value of the new cross-correlation energy function is not greater than the 0.85 times of the minimum peak value of the old cross-correlation energy function, the alteration of the pixel value won't be accepted and the process returns to the step 3.

5. Calculate the difference of energy functions, which is  $\Delta E$  and expressed as

$$\Delta E = E_{new} - E_{old} \tag{13}$$

6. If  $\Delta E \leq 0$ , accept the level number in the new reference function  $h(x, y)$ , set  $E_{new}$  to be the next time calculated system temperature  $T$ , and starting point  $E_{old}$ .

7. If not, utilize  $P(\Delta E)$  to calculate the probability. If  $P(\Delta E)$  is greater than a random number  $r$  in the range between 0 and 1, and then accept the alteration of the pixel value.

8. Check whether all pixels have been operated, move to the next step. Otherwise move to step 4.

9. Record the value of energy function. If the normalized standard deviation of energy for the last ten times is smaller than 0.03, and then move to step 10. Otherwise reduce  $kT = 0.9 * kT$ , and move to step 3.

10. Repeat previous steps by using 9, 17 and 129 different levels.

### IV. RESULTS

According to simulated annealing algorithm, we execute numerical simulation with computers, and then records each cycle of the minimum energy function  $E$ . The SA processes will be terminated when last ten times the normalized standard deviation  $\sigma$  of energy function is smaller than 0.03 by supposing that the outcome achieves convergence.

Fig. 3 shows the optimal reference functions using 129 levels. Fig. 4 shows the three-dimensional profiles of the correlation output plane. Fig. 5 shows CPI curve versus the rotation angle for the training, non-training and non-target images. Figs. 6 (a) and 6 (b) show the ACPE and APSR versus SNR values from 1 to 10 dB by using 9, 17 and 129 different levels. Results show that the optoelectronic pattern recognition performance with simulated annealing is feasible.

V. CONCLUSIONS

In this paper, we have proposed a MZJTC with simulated annealing for pattern recognition. In order to yield a better reference function, we use both of MACE and SA for seeking minimum average energy. We discuss different levels of reference functions for testing recognition ability. The recognition effect is quite appealing. In the future, we can attempt to modify SA. If we can effectively control the convergence and convergence rate, it will somehow improve the reliability of image recognition.

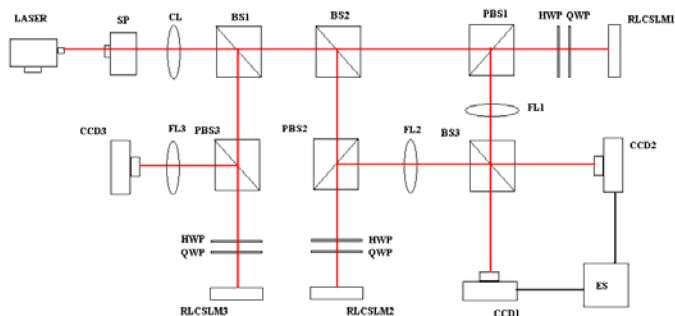


Fig. 1 Mach-Zehnder JTC structure



Fig. 3 Reference function yielded by simulated annealing.

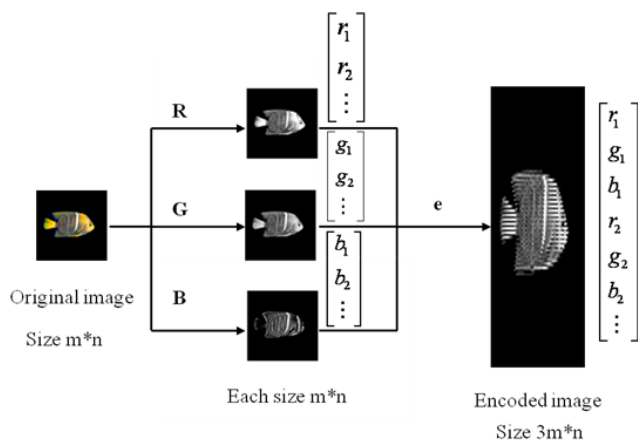


Fig. 2 Flow chart of encoded image.

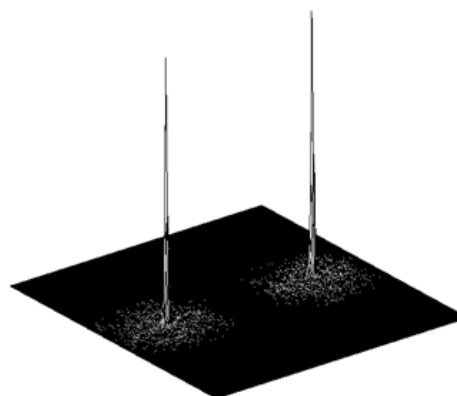


Fig. 4 Correlation output plane of NZJTC

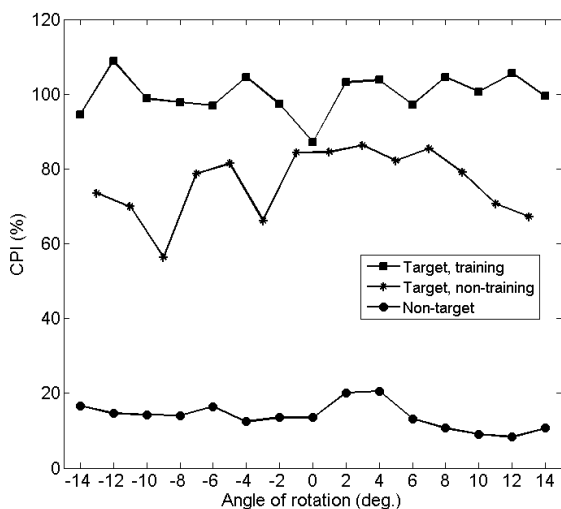


Fig. 5 CPI versus rotation angle from  $-14^\circ$  to  $14^\circ$

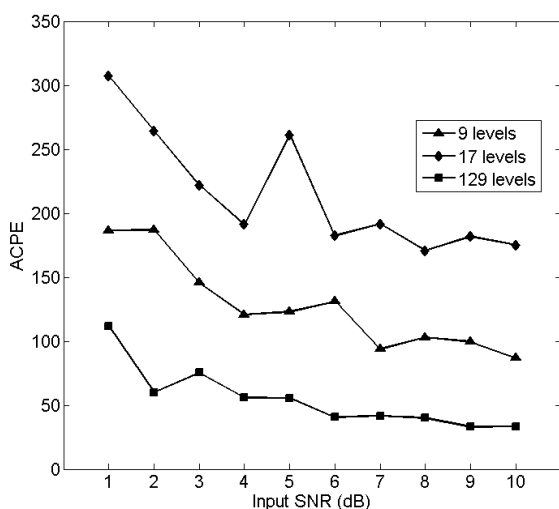


Fig. 6 (a) ACPE versus SNR from 1 to 10 dB.

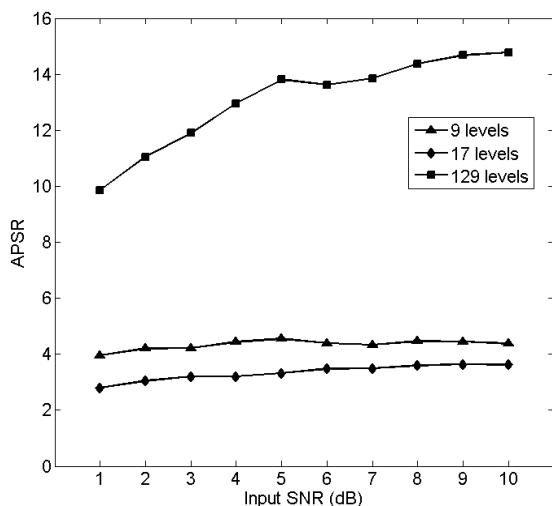


Fig. 7 (b) APSR versus SNR from 1 to 10 dB.

## REFERENCES

- [1] A. VANDER LUGT. "Signal detection by complex spatial filtering." *IEEE transactions on information theory*, vol. 10, 2, pp. 139-145, 1964.
- [2] C. S. Weaver and J. W. Goodman, "A Technique for Optically Convolver Two Functions," *Appl. Opt.*, vol. 5, pp. 1248-1249, 1966.
- [3] G. Lu, et al., "Implementation of a non-zero-order joint-transform correlator by use of phase-shifting techniques," *Appl. Opt.*, vol. 36, pp. 470-483, 1997.
- [4] C. Li, S. Yin and F. T. S. Yu, "Nonzero-order joint transform correlator", *Opt. Eng.*, vol. 37, pp. 58-65, 1998.
- [5] C. Cheng and H. Tu, "Implementation of a nonzero-order joint transform correlator using interferometric technique," *Opt. Rev.*, vol. 9, pp. 193-196, 2002.
- [6] Y. Lin, C. Chen, C. Lee "Mach-Zehnder joint transform correlator with multi-channel quantized reference functions for color pattern recognition," *Opt. Commun.*, vol. 266, pp. 111-116, 2006
- [7] C. Lee, C. Chen, "Colour pattern recognition based on a multi-channel Mach-Zehnder joint transform correlator with multi-level quantized reference functions," *Journal of Modern Optics*, vol. 55, pp. 409-422, 2008.
- [8] S. Kirkpatrick, et al., "Optimization by Simulated Annealing," *Science*, vol. 220, pp. 671-680, 1983.
- [9] B. V. K. V. Kumar and L. Hassebrook, "Performance measures for correlation filters," *Appl. Opt.*, vol. 29, pp. 2997-3006, 1990.
- [10] Chewei Chen and Chulung Chen, "A Mach-Zehnder joint transform correlator with the simulated annealing algorithm for pattern recognition," *Opt. Commun.*, vol. 284, pp. 3946-3953, 2011.